# Supporting information

## Evaluation of Carbonized Corncobs for Removal of Microcystins and Nodularin-R from Water

Hasaruwani S. Kiridena [a], Sharmila I. Thenuwara [a], Manjula M. Kandage [a], Norman Peiffer [b], Michal Marszewski [a], and Dragan Isailovic [a,*]

[a] Department of Chemistry and Biochemistry, University of Toledo, Toledo, OH 43606, USA
[b] The Andersons, Maumee, OH 43537, USA

*Corresponding Author:
Dragan Isailovic
Department of Chemistry and Biochemistry
MS 602
University of Toledo
Toledo, OH 43606

Email: Dragan.Isailovic@utoledo.edu
Phone: +1 (419) 530-5523

# Table of Contents

**Sample preparation by solid-phase extraction (SPE) and analysis by UHPLC-MS**

Sep-Pak C18 cartridge was conditioned with 2 mL of methanol:water (90:10 v/v) containing 0.1% formic acid and equilibrated with 2 mL of 0.1% formic acid. The sample was loaded onto the cartridge and washed with 0.1% formic acid. MCs and NOD-R were eluted with 2 mL of acetonitrile: water (90:10 v/v) containing 0.1% formic acid. Finally, the eluent was evaporated using a vacuum concentrator. Prior to LC-MS analysis, pre-concentrated samples were reconstituted in 200 μL of acetonitrile: water (35:65, v/v) containing 0.1% formic acid.

The binary gradient of 0.1% formic acid in water (mobile phase A) and acetonitrile with 0.1% formic acid (mobile phase B) was used. The C18 column was equilibrated with 10% B before the initial injection. The flow rate was 0.667 mL/min and 20 μL of the sample was injected per run. The gradient started at 10% B and was increased to 25% B in 0.03 minutes, to 46.4% B in 1 minute, and to 95% B in 2.7 minutes. Then it was decreased to 10% B in 3.32 minutes and maintained for 2.68 minutes. The total run time was 6 minutes. Heated-ESI source in positive ion mode was used for ionization. A quadrupole was used for selected ion monitoring (SIM). MS and MS/MS were performed simultaneously and higher-energy collision-induced dissociation (HCD) was used to fragment MC and NOD-R precursor ions. The Orbitrap mass analyzer was used to measure m/z of precursor ions, and fragment ions were analyzed with a linear ion trap mass analyzer. The ADDA fragment ion $[C_6H_5-CH_2CH(OCH_3)]^+$ at m/z 135.08 was used for the identification of MCs and NOD-R in MS/MS mode. Seven SIM channels were monitored (with mass accuracy < 3 ppm) when using a mixture of six MCs and NOD-R: six for the singly-protonated ions ($[M+H]^+$) of MC-LR (m/z 995.56), MC-YR (m/z 1045.54), MC-LA (m/z 910.49), MC-LW (m/z 1025.53), MC-LF (m/z 986.52), and NOD-R (m/z 825.45) and one for the doubly-protonated ($[M+2H]^{2+}$) ion of MC-RR (m/z 519.79). All samples were analyzed in triplicate. The quantification of MCs and NOD-R was performed using an LC-MS external calibration protocol. The calibration curve was plotted in the concentration range from 0.25 to 100 μg/L.
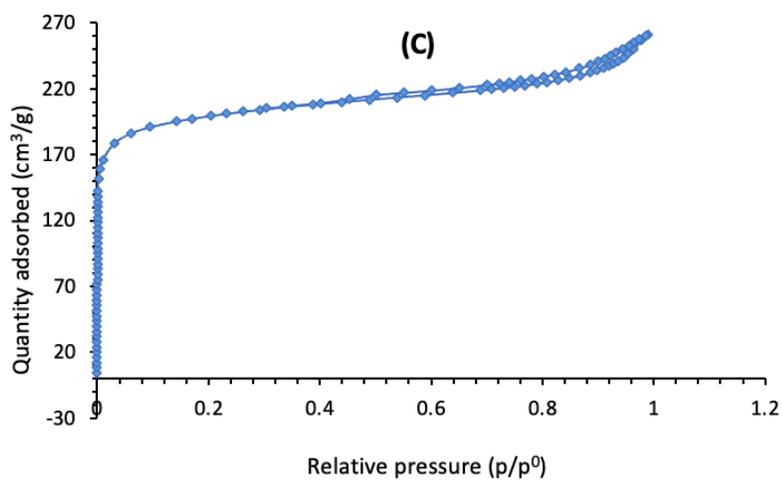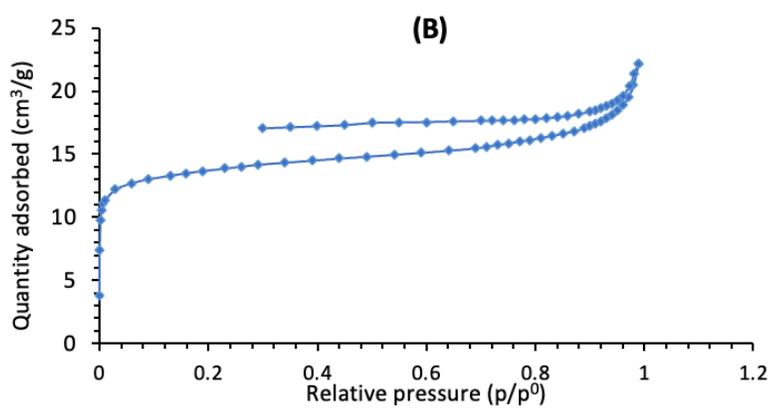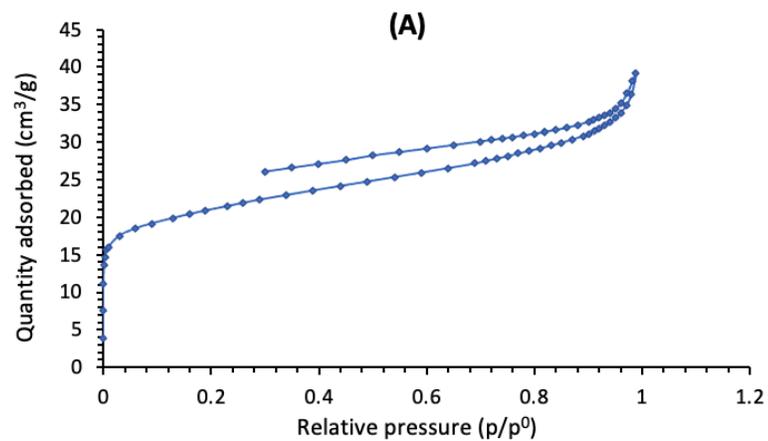
Figure S1: Surface area and porosity measurements of (A) S−3, (B) S−4, and (C) commercial AC.
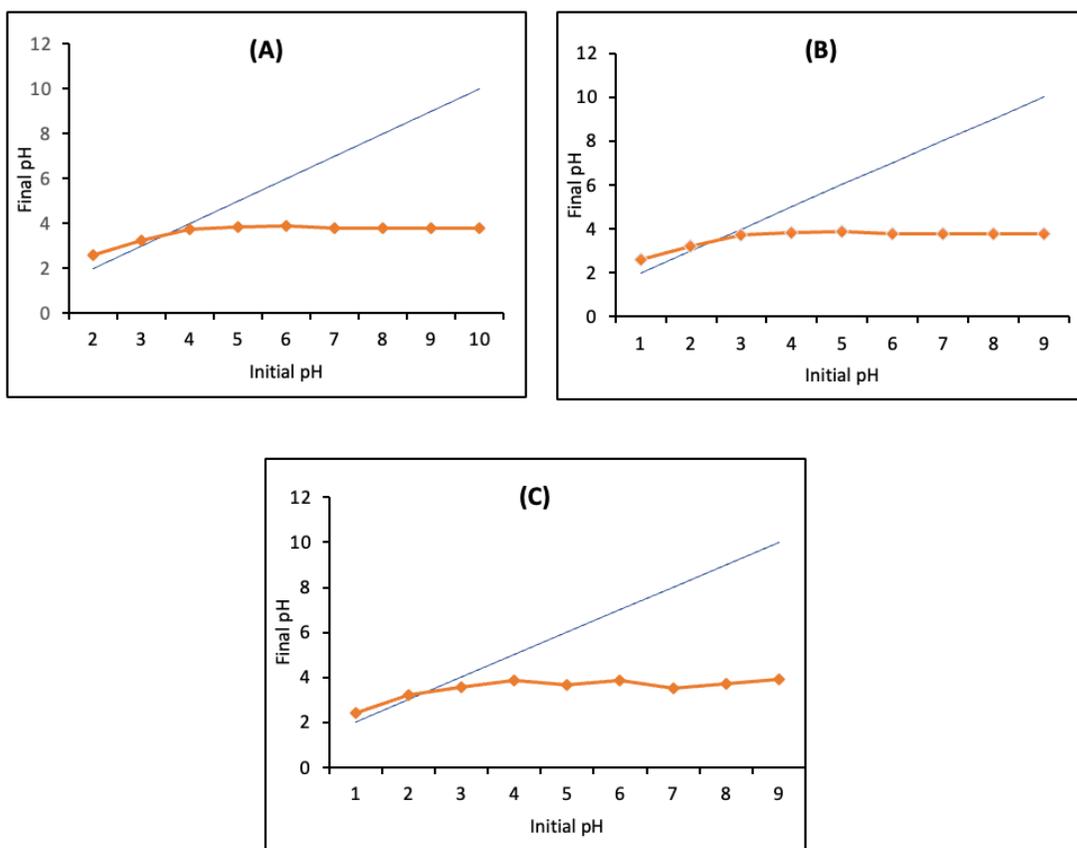
Figure S2: pH$_{PZC}$ of (A) H$_3$PO$_4$−AC, (B) S−3, and (C) S−4.

Table S1: Net charges of MCs and NOD-R at neutral pH

| MCs/NOD-R | Theoretical m/z | Dominant charged species[*] | Net charge at natural water pH |
|---|---|---|---|
| MC-RR | 519.7902 | Glu(R-COO$^-$), MeAsp(R-COO$^-$), Arg(R=NH$_2^+$)$_2$ | 0 |
| NOD-R | 825.4506 | Glu(R-COO$^-$), MeAsp(R-COO$^-$), Arg(R=NH$_2^+$) | -1 |
| MC-YR | 1045.5353 | Glu(R-COO$^-$), MeAsp(R-COO$^-$), Arg(R=NH$_2^+$) | -1 |
| MC-LR | 995.5561 | Glu(R-COO$^-$), MeAsp(R-COO$^-$), Arg(R=NH$_2^+$) | -1 |
| MC-LA | 910.4921 | Glu(R-COO$^-$), MeAsp(R-COO$^-$) | -2 |
| MC-LW | 1025.5343 | Glu(R-COO$^-$), MeAsp(R-COO$^-$) | -2 |
| MC-LF | 986.5234 | Glu(R-COO$^-$), MeAsp(R-COO$^-$) | -2 |

[*]R in this column represents the side chain of an amino acid
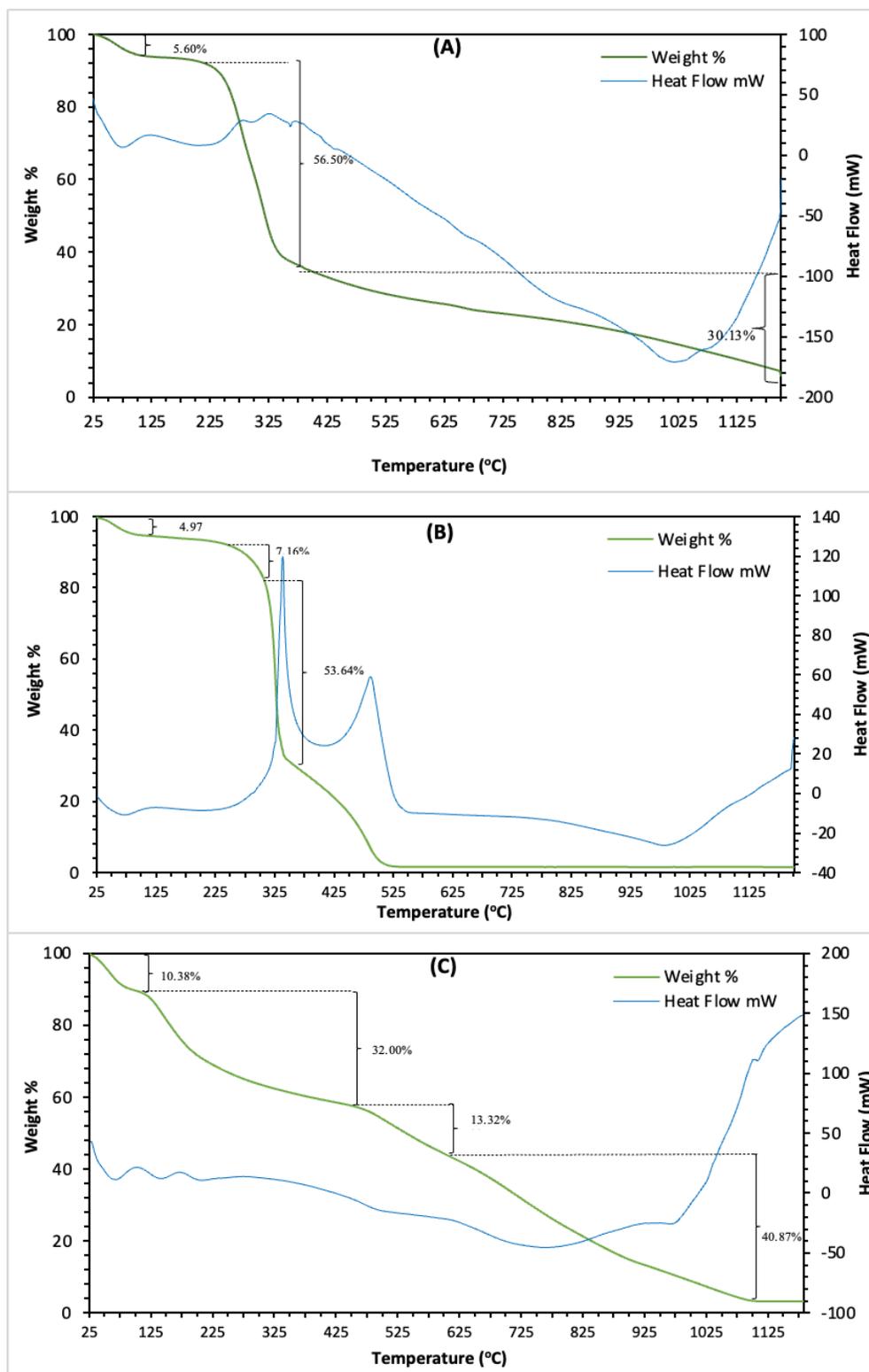
Figure S3: Thermo gravimetric analysis of (A) raw corncob, (B) HCl–refluxed corncob, and (C) H₃PO₄–impregnated corncob.
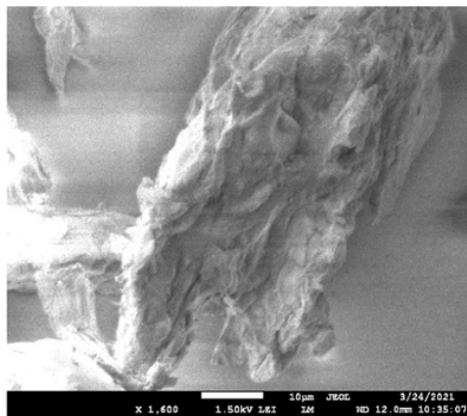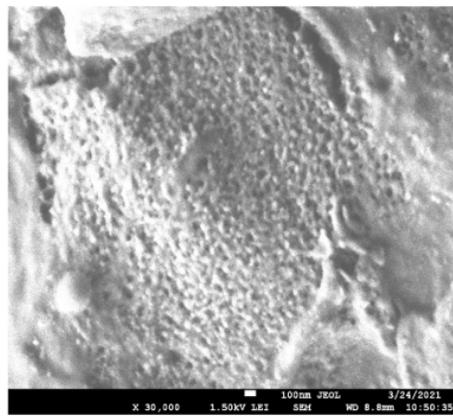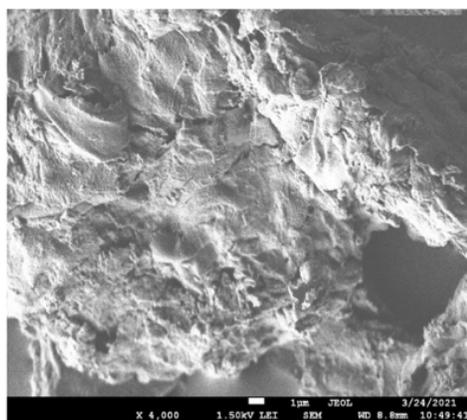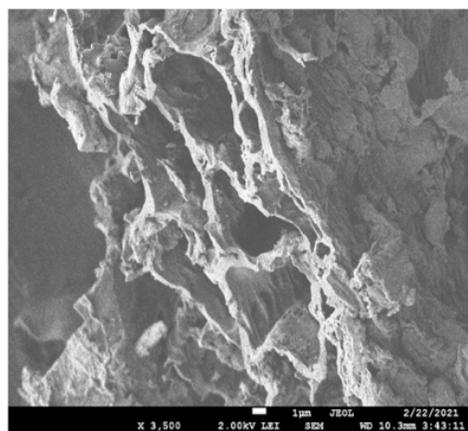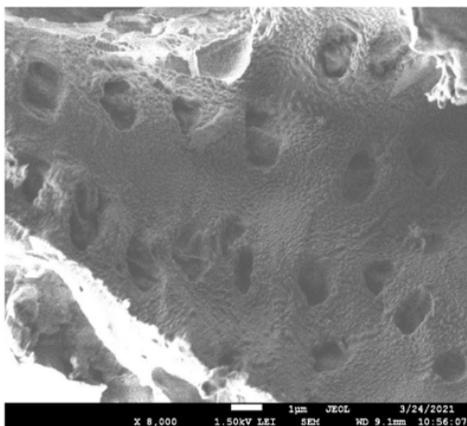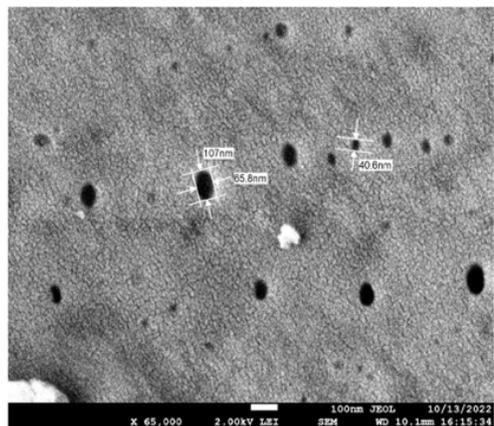
Figure S4: SEM images of (A) raw corncob, (B, C) HCl-refluxed corncobs, (D) S−3, (E) S−4, and (F) $H_3PO_4$−AC.

The SEM images in Figure S4 display the surface features of raw corncobs, biochar, and $H_3PO_4$−AC. They confirm that the external surfaces of S−3, S−4, and $H_3PO_4$−AC contain well-developed cavities with different diameters distributed over the surfaces. These cavities increase the surface area of the sorbent and enhances the uptake of MCs and NOD-R from aqueous solutions.
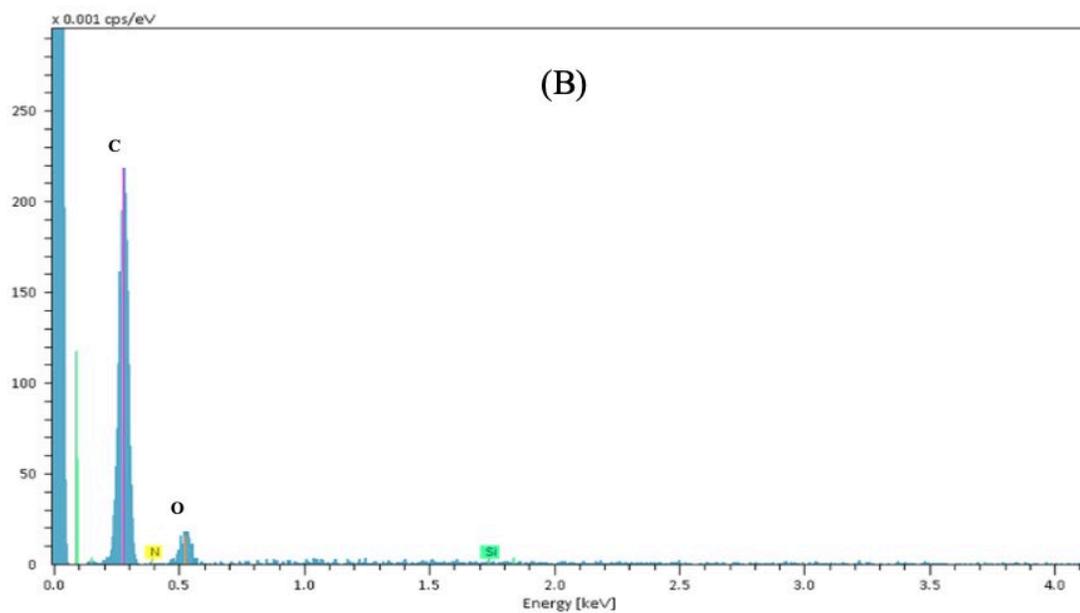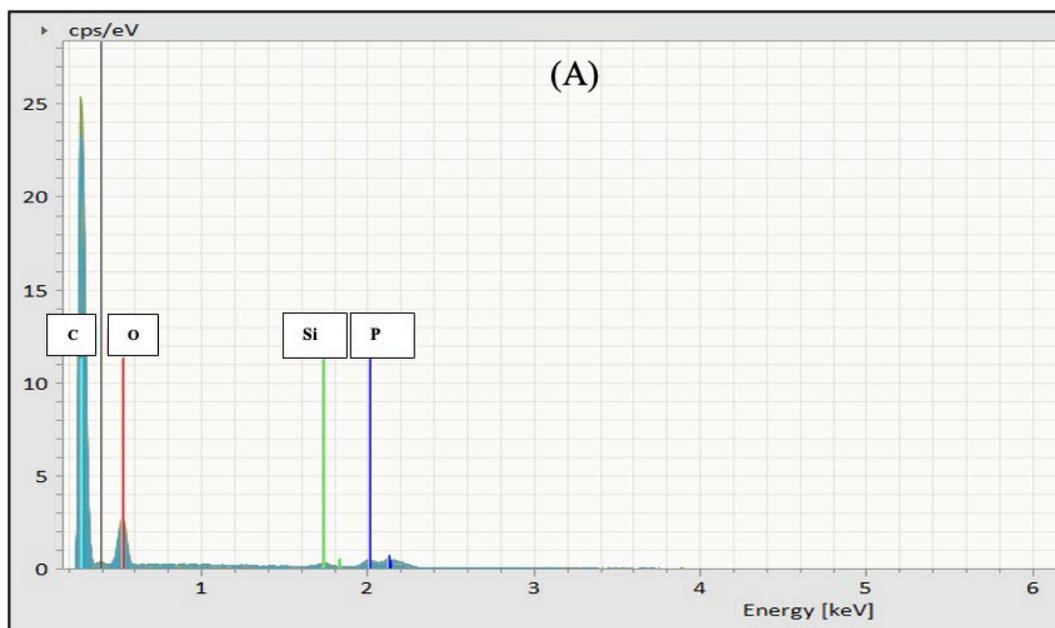
Figure S5: SEM-EDS spectra of (A) H$_3$PO$_4$−AC and (B) S−3

The EDS elemental analysis confirmed that both S−3 and H$_3$PO$_4$−AC (Fig. S5) are composed mostly of carbon, and oxygen, with some trace elements. H$_3$PO$_4$−AC contains some amount of P, and this could be due to the so-called "phosphate skin" produced by phosphoric acid. This phosphate skin protects the internal structure of carbon from excessive burn-off that leads to surface area decrease during the activation step.
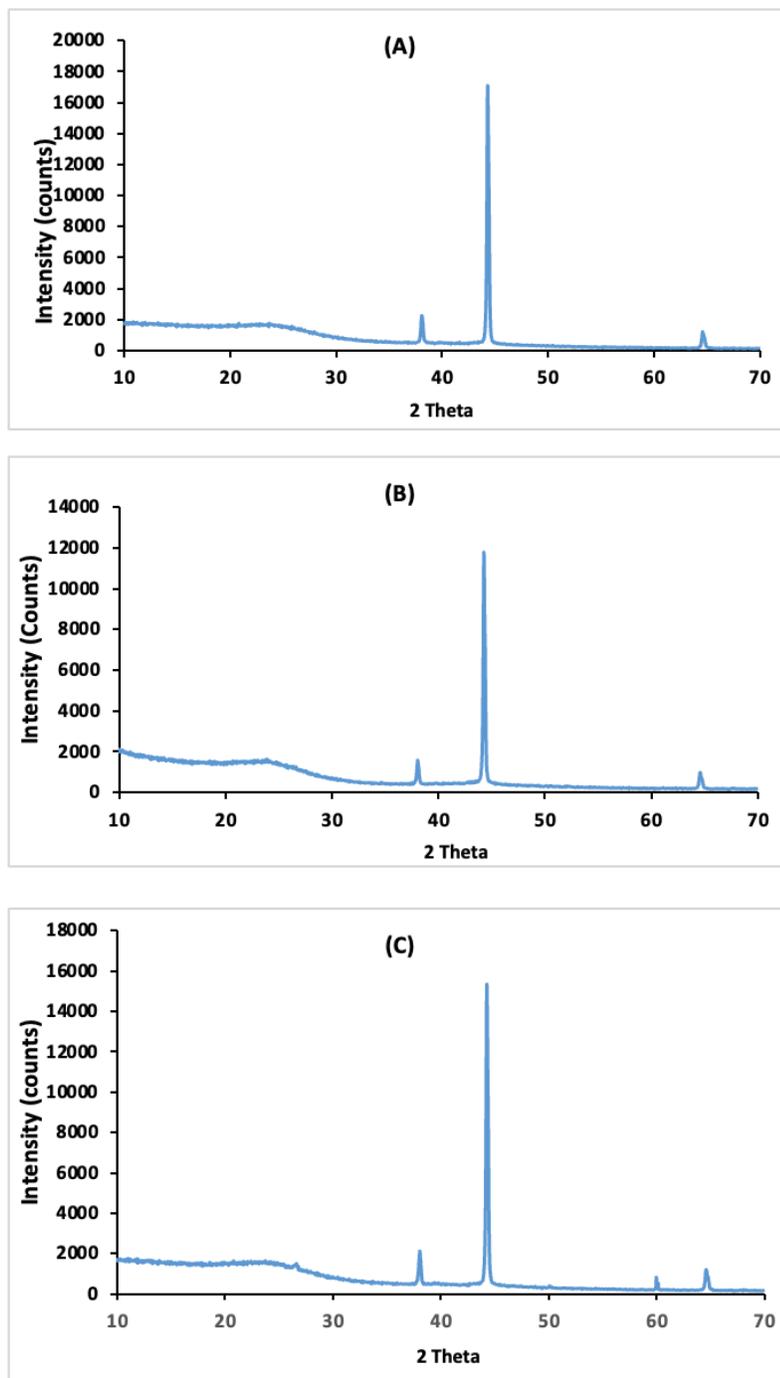
Figure S6: PXRD patterns of (A) S−3 (B) H$_3$PO$_4$−AC, and (C) S−4
(Particle size < 250 microns)
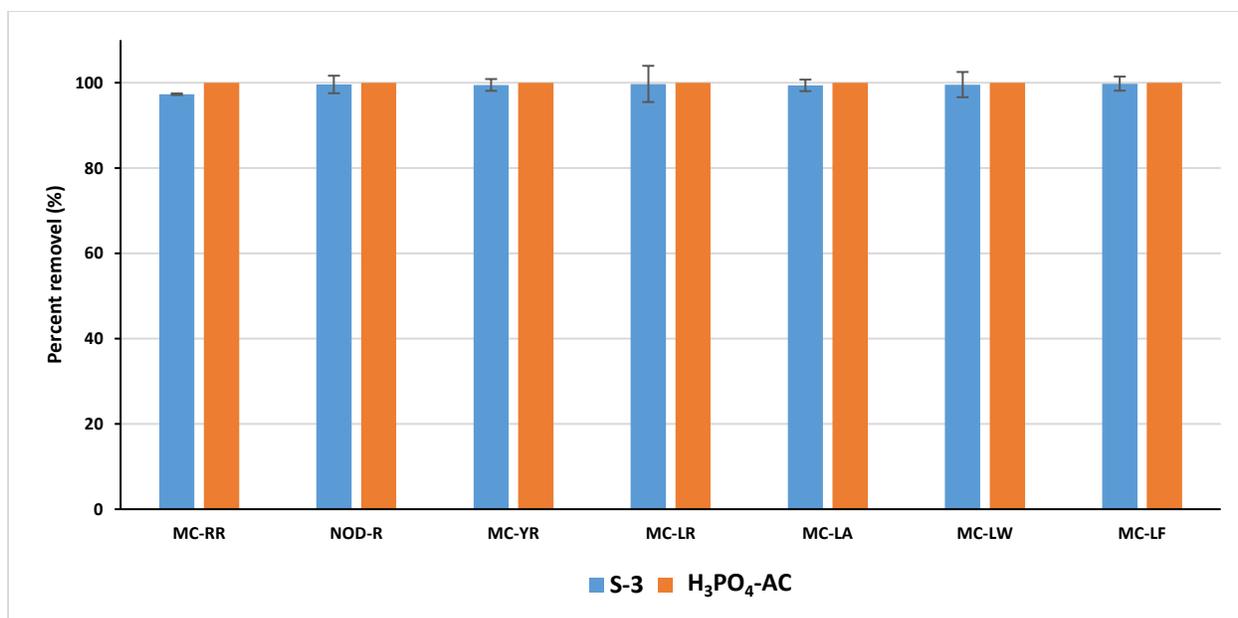
Figure S7: Percent removal of six MCs and NOD-R using S−3 and H₃PO₄−AC in suspension mode (n=3). The initial concentration of each MC and NOD-R, sorbent amount, and solution volume were 1000 µg/L, 50 mg, and 1 mL, respectively.

Table S2: Concentrations of MCs in lake water collected during HAB in 2020, and their percent removal using carbonized corncobs and commercial AC.

| MCs | Concentration (μg/L) | Percent removal (%) | | | |
|---|---|---|---|---|---|
| | | S−3 | S−4 | $H_3PO_4$−AC | Commercial AC |
| MC-RR | 276.53 (±10.84) | 100 | 100 | 100 | 100 |
| MC-YR | 25.64 (±0.33) | 100 | 100 | 100 | 100 |
| MC-LR | 131.50 (±0.64) | 100 | 100 | 100 | 100 |
| MC-LA | 4.84 (±0.16) | 100 | 100 | 100 | 100 |

(S−3: HCl-refluxed and heated to 300ºC, S−4: HCl-refluxed and heated to 350ºC.)

Table S3: Concentrations of MCs in lake water collected during HAB in 2021, and their percent removal using carbonized corncobs and commercial AC.

| MCs | Concentration (μg/L) | Percent removal (%) | | | |
|---|---|---|---|---|---|
| | | S−3 | S−4 | $H_3PO_4$−AC | Commercial AC |
| MC-RR | 1.30 (±0.01) | 100 | 100 | 100 | 100 |
| MC-LR | 0.07( ±0.05) | 100 | 100 | 100 | 100 |

(S−3: HCl-refluxed and heated to 300ºC, S−4: HCl-refluxed and heated to 350ºC.)

Table S4: Concentrations of MCs in lake water collected during HAB in 2022, and their percent removal using carbonized corncobs and commercial AC.

| MCs | Concentration (μg/L) | Percent removal (%) | | | |
|---|---|---|---|---|---|
| | | S−3 | S−4 | $H_3PO_4$−AC | Commercial AC |
| MC-RR | 240.97 (±1.70) | 100 | 100 | 100 | 100 |
| MC-YR | 42.78 (±0.30) | 100 | 99.80 (±2.55) | 100 | 100 |
| MC-LR | 126.01 (±0.50) | 99.56 (±1.40) | 98.97 (±2.56) | 100 | 100 |
| MC-LA | 4.20 (±3.54) | 80.90 (±2.07) | 76.33 (± 1.78) | 100 | 100 |

(S−3: HCl-refluxed and heated to 300ºC, S−4: HCl-refluxed and heated to 350ºC.)
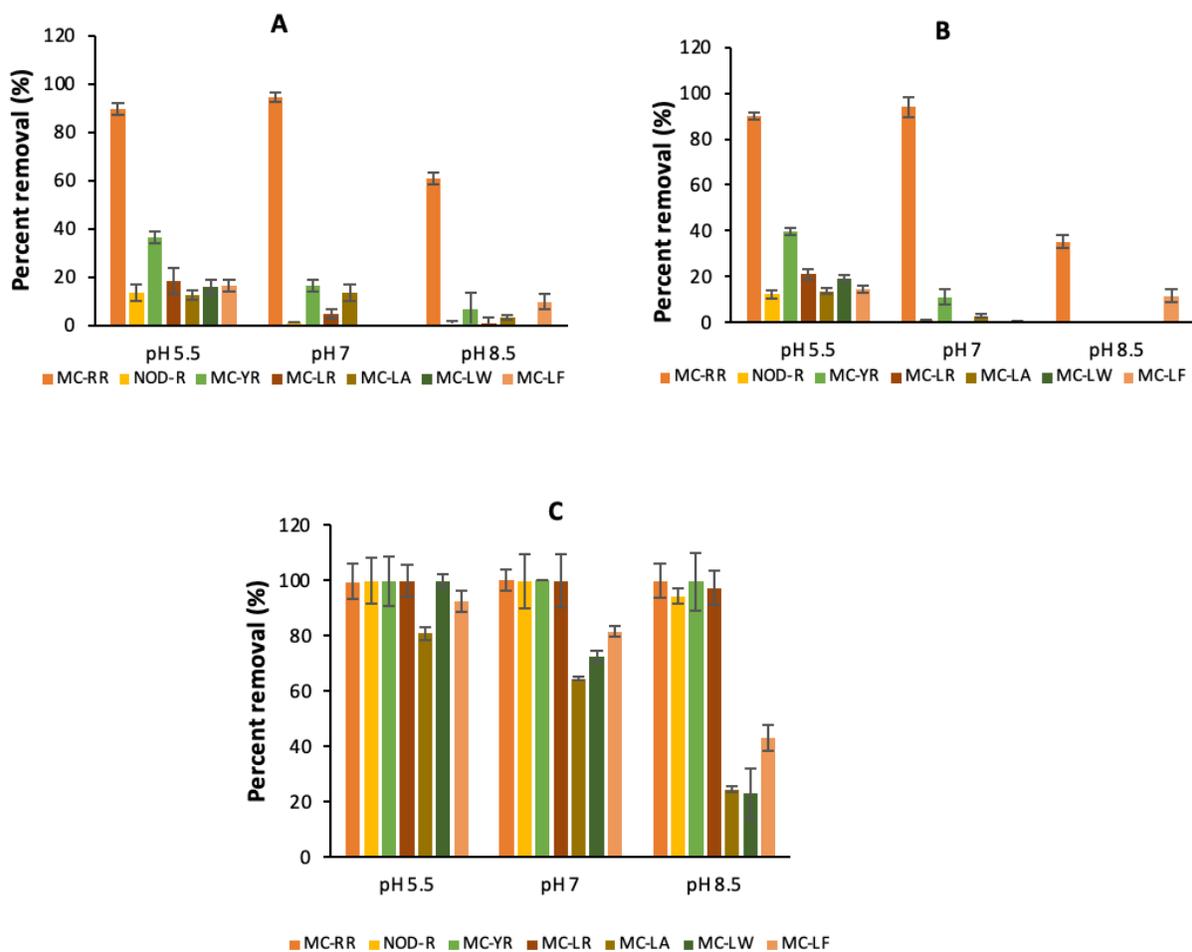
Figure S8: Percent removal of six MCs and NOD-R at different pH conditions using (A) S−3, (B) S−4, and (C) H₃PO₄−AC (n=3). The initial concentration of each MC and NOD-R, sorbent amount, and solution volume were 50 μg/L, 0.5 mg, and 1 mL, respectively.
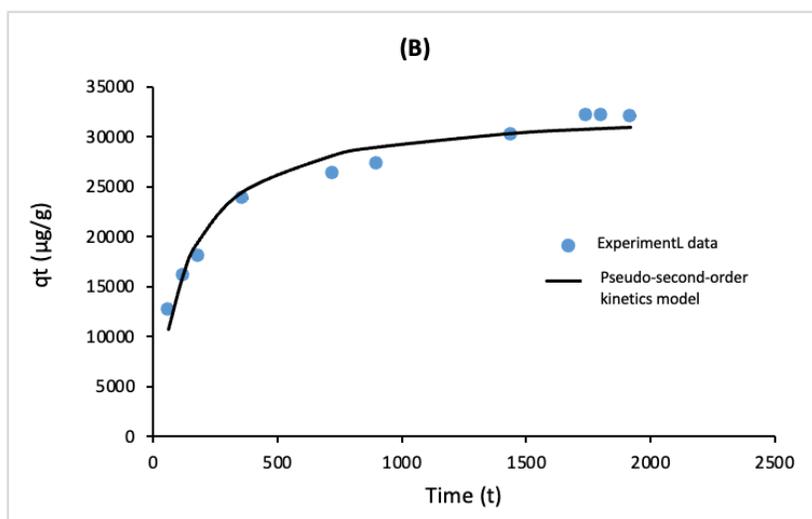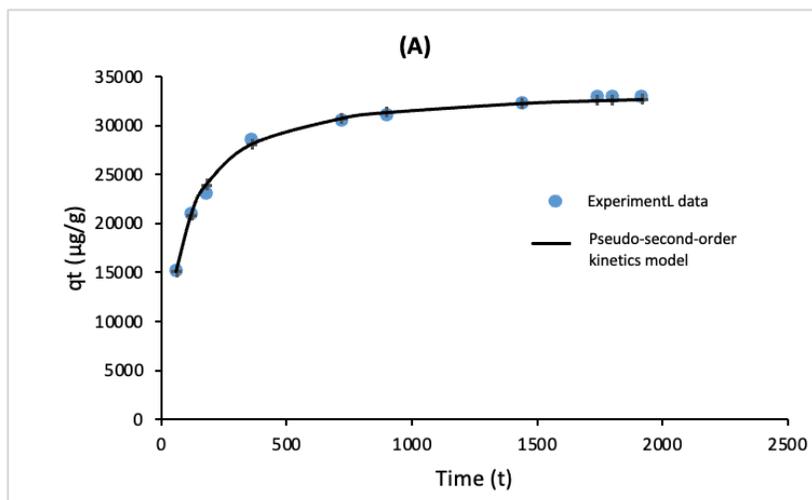
Figure S9: Non-linear plots of pseudo-second-order kinetics models for the adsorption of (A) MC-LR and (B) NOD-R onto $H_3PO_4$−AC. Error bars represent ± one standard deviation (n=3). The initial concentrations, amount of sorbent, and volume of solution were 2000 μg/L, 0.5 mg, and 10 mL, respectively.
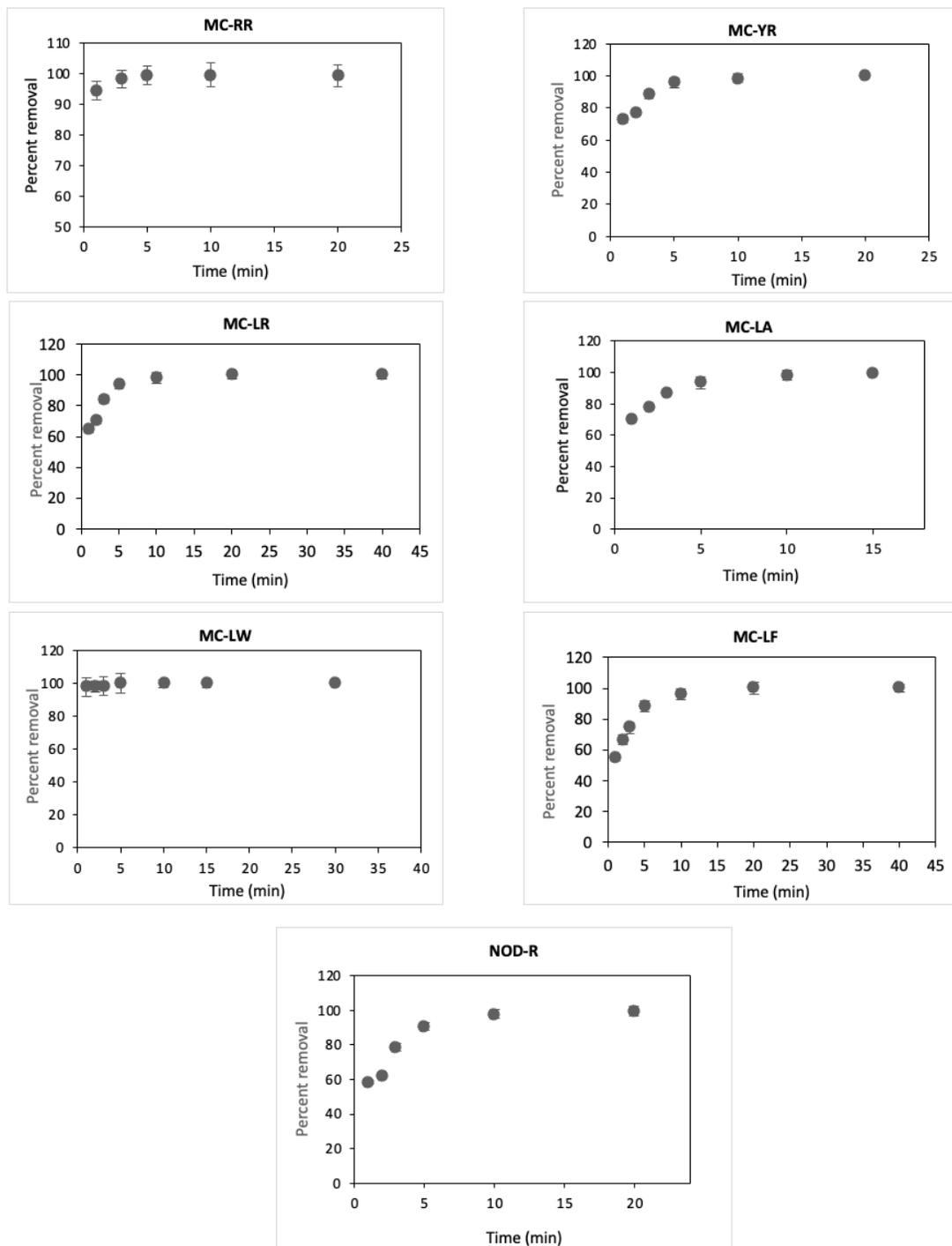
Figure S10: Sorption kinetics of six MCs and NOD-R. Error bars represent ± one standard deviation (n=3). The initial concentrations, amount of sorbent, and volume of solution were 20 μg/L of each MC and NOD-R, 20 mg, and 30 mL, respectively.

Kinetics experiments showed that the removal of MCs and NOD-R from water using treated corncobs is a rapid process. Twenty milligrams of corncob-based activated carbon was able to remove >95% of MC-RR, NOD-R, MC-YR, MC-LR, MC-LW, >80% of MC-LF and >68% of MC-LA in the first minute, from a 30 mL solution of six MCs and NOD-R (20 µg/L each). Removal was improved with an increase in adsorption time, and maximum removal (>95% for all MCs and NOD-R) occurred after 5 minutes.

Table S5: Adsorption capacities reported by previous work.

| Targeted MCs | Material | Sorption conditions | Sorption capacity | Reference |
|---|---|---|---|---|
| MC-LR | Wood-based powdered AC (PAC) | pH 5.2-6.6 | 280 µg/mg | (Donati et al., 1994) |
| MC-LR | Charcoal based PACs | pH 5.2-6.6 | 116, 75 and 70 µg/mg | (Donati et al., 1994) |
| MC-LR | Coconut shell-based PACs | pH 5.2-6.6 | 20 and 40 µg/mg | (Donati et al., 1994) |
| MC-LR | *Moringa oleifera* Lam. Seeds derived biochar | pH 3, Room temperature | >92 µg/mg | (Yasmin et al., 2019) |
| MC-LR | Rubber wood based based AC | 303 K | 296 µg/mg | (Hena et al., 2014) |
| MC-LR | Sugarcane bagasse-AC fibers | pH 6 -8.5 | 161.3 µg/mg | (Albuquerque Júnior et al., 2008) |
| MC-LR | Pinewood-based AC fibers | pH 6 -8.5 | 200 µg/mg | (Albuquerque Júnior et al., 2008) |
| MC-LR | Kentucky bluegrass-derived biochar | pH 6 | 2769 µg/g | (Song et al., 2021) |
| MC-LR | Giant reed-derived biochars | pH 5 | 42 µg/mg | (Liu et al., 2018) |
| MC-RR, MC-YR, MC-LR, MC-LA, MC-LW, and MC-LF | Rice husk-based biochar | pH 7, Room temperature | 586 µg/g | (Palagama et al., 2019) |
| MC-LR | Bermudagrass based biochar | pH 6 | 10.2 µg/mg | (Zeng and Kan, 2021) |